Supplementary Information

Designing polymer nanocomposites with high energy-density using machine learning

Zhong-Hui Shen*, Zhi-Wei Bao, Xiao-Xing Cheng, Bao-Wen Li, Han-Xing Liu, Yang Shen, Long-Qing Chen, Xiao-Guang Li*, Ce-Wen Nan*

*Corresponding author. E-mail:

zhshen@whut.edu.cn (Z. H. Shen)

lixg@ustc.edu.cn (X. G. Li)

cwnan@mail.tsinghua.edu.cn (C. W. Nan)

This PDF file includes:

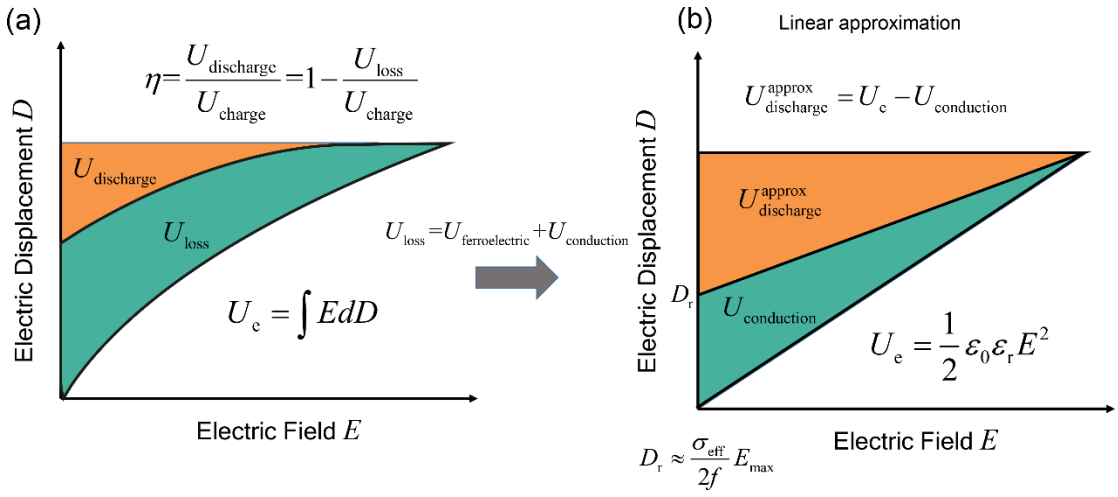

Supplementary Figure 1 Schematic diagram of calculating the energy density of a dielectric from ferroelectric loop.

Supplementary Table 1 Summary of the maximal energy density and breakdown strength for this work and some state-of-the-art two-phase polymer nanocomposites

Polymer Matrix	Nanofiller	Breakdown Strength (MV/m)	Maximal Discharged Energy Density (J/cm^3)
P(VDF-HFP)	$BaTiO_3$ nanoparticle	585.5[1]	16.5
P(VDF-HFP)	$BaTiO_3$ nanofiber	602[1]	18.5
P(VDF-HFP)	$BaTiO_3$ nanoparticle	540[2]	13.0
P(VDF-HFP)	$Pb_{0.97}La_{0.02}(Zr_{0.5}Sn_{0.38}Ti_{0.12})O_3$ nanoparticle	316[3]	12.5
PVDF	$BaTiO_3$ nanoparticle	450[4]	10
P(VDF-HFP)	SiO_2 nanoparticle	550[5]	13
P(VDF-HFP)	Al_2O_3 nanoparticle	600[5]	15.8
P(VDF-HFP)	TiO_2 nanoparticle	500[5]	12.5
PVDF	$BaTiO_3$ nanoparticle	470[6]	18.8
PVDF	$PbZr_{0.2}Ti_{0.8}O_3$ nanowire	40[7]	1.28
P(VDF-TrFE-CFE)	$BaTiO_3$ nanofiber	300[8]	10.48
PVDF	MoS_2 nanosheet	200[9]	4.1
PVDF	$NaNbO_3$ nanoplatelet	400[10]	13.5
PVDF	TiO_2 nanosheet	650[11]	21.1
PVDF	$Ba_{0.2}Sr_{0.8}TiO_3$ nanowire	450[12]	14.86
P(VDF-HFP)	$BaTiO_3$ nanoparticle	164[13]	3.2
P(VDF-TrFE-CFE)	BN nanosheet	610[14]	20.3
P(VDF-HFP)	TiO_2 nanowire	530[15]	11.48
P(VDF-HFP)	$Ca_2Nb_3O_{10}$ nanosheet	853*	35.9

*: this work

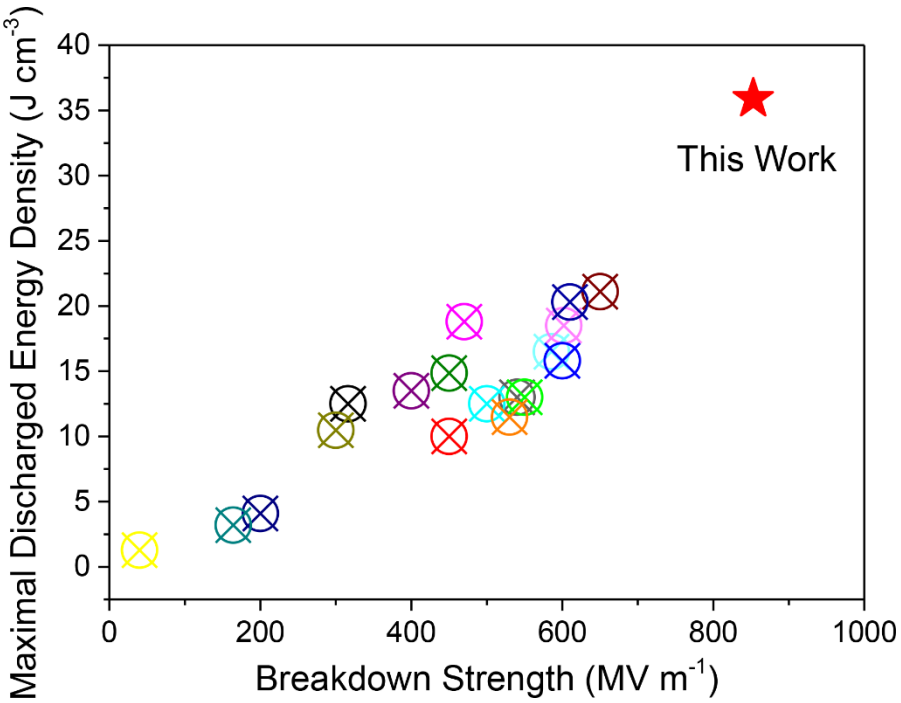

Supplementary Figure 2 Comparisons of the maximal energy density and breakdown strength for this work and some state-of-the-art two-phase polymer nanocomposites.

Supplementary Table 2 The material parameters used in the prediction of machine learning

Perovskite Nanosheet	Permittivity	Out of plane Electrical Conductivity (S m^{-1})	Out of plane Electron Mobility (cm^2 V^{-1} s^{-1})
$Sr_2Ta_3O_{10}$	175	1×10^{-15}	1×10^{-14}
$Ca_2Nb_3O_{10}$	213	1×10^{-15}	1×10^{-14}
$LaNb_2O_7$	50	1×10^{-15}	1×10^{-14}
$Sr_2Nb_3O_{10}$	240	1×10^{-15}	1×10^{-14}
$Ca_2Ta_3O_{10}$	47	1×10^{-15}	1×10^{-14}

※ Due to the lack of accurate electrical conductivity and electron mobility in experiments, a constant empirical value is given in this prediction to represent the high insulativity of perovskite nanosheets.

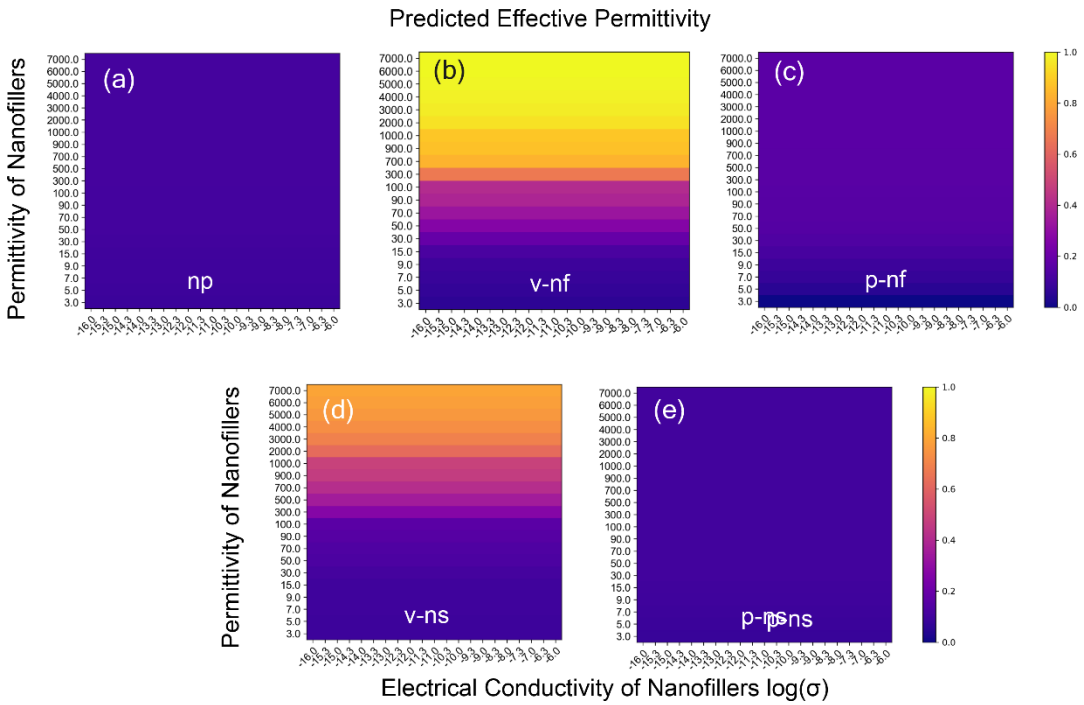

Supplementary Figure 3 Predicted effective permittivity of polymer nanocomposites with different nanofillers (a) Nanoparticle (b) Vertical Nanofiber (c) Parallel Nanofiber (d) Vertical Nanosheet (e) Parallel Nanosheet.

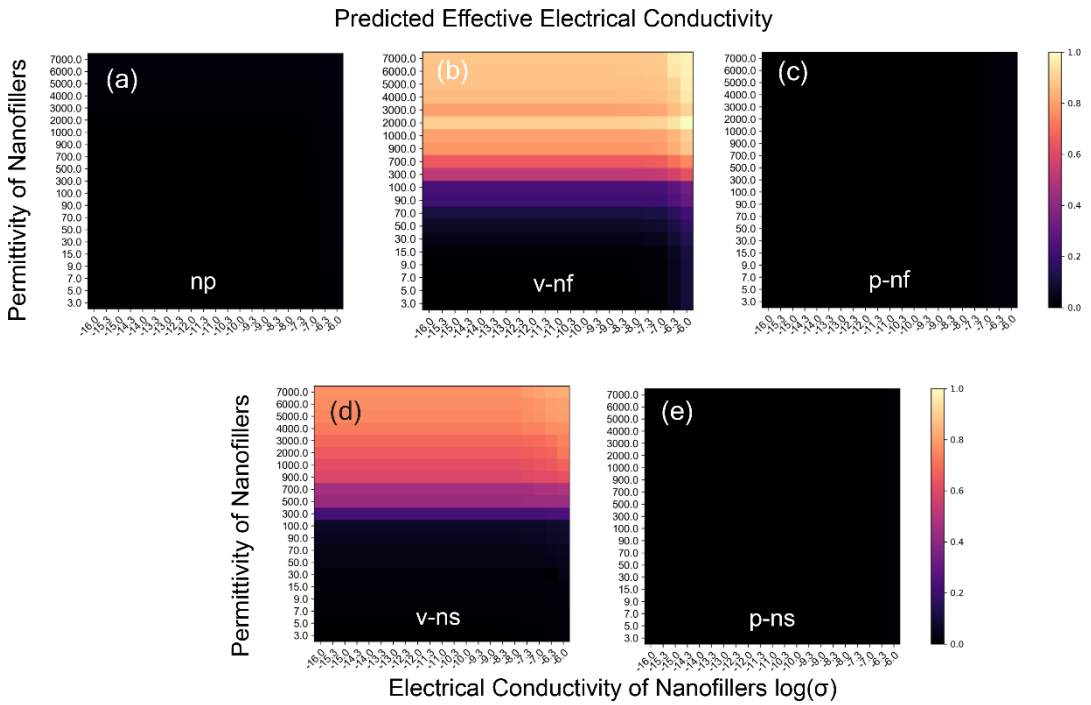

Supplementary Figure 4 Predicted effective electrical conductivity of polymer nanocomposites with different nanofillers (a) Nanoparticle (b) Vertical Nanofiber (c) Parallel Nanofiber (d) Vertical Nanosheet (e) Parallel Nanosheet..

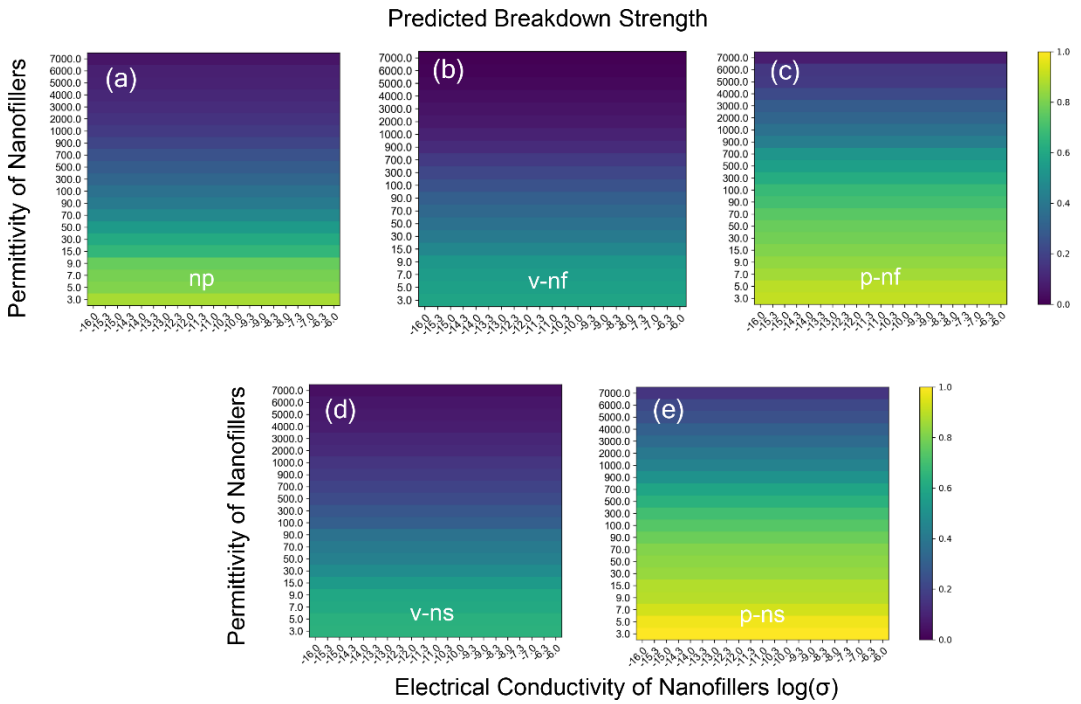

Supplementary Figure 5 Predicted breakdown strength of polymer nanocomposites with different nanofillers (a) Nanoparticle (b) Vertical Nanofiber (c) Parallel Nanofiber (d) Vertical Nanosheet (e) Parallel Nanosheet.

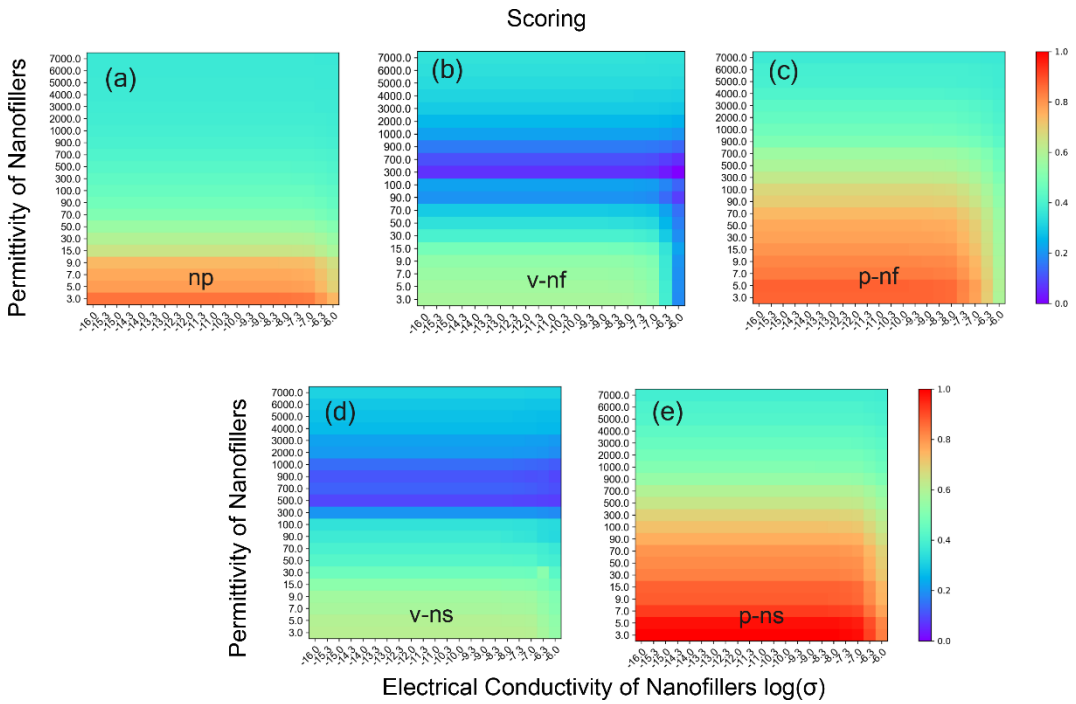

Supplementary Figure 6 Scoring of polymer nanocomposites with different nanofillers (a) Nanoparticle (b) Vertical Nanofiber (c) Parallel Nanofiber (d) Vertical Nanosheet (e) Parallel Nanosheet.

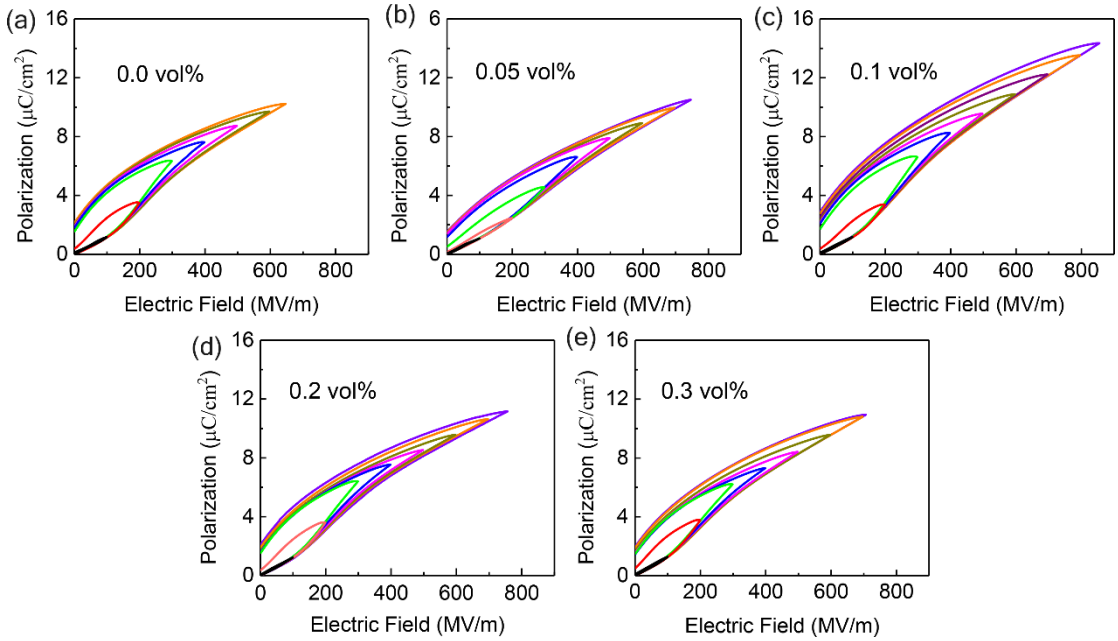

Supplementary Figure 7 Ferroelectric loops of polymer nanocomposite P(VDF-HFP)/$Ca_2Nb_3O_{10}$ with different volume fraction (a) 0.0vol% (b) 0.05vol% (c) 0.1% (d) 0.2vol% (e) 0.3vol%

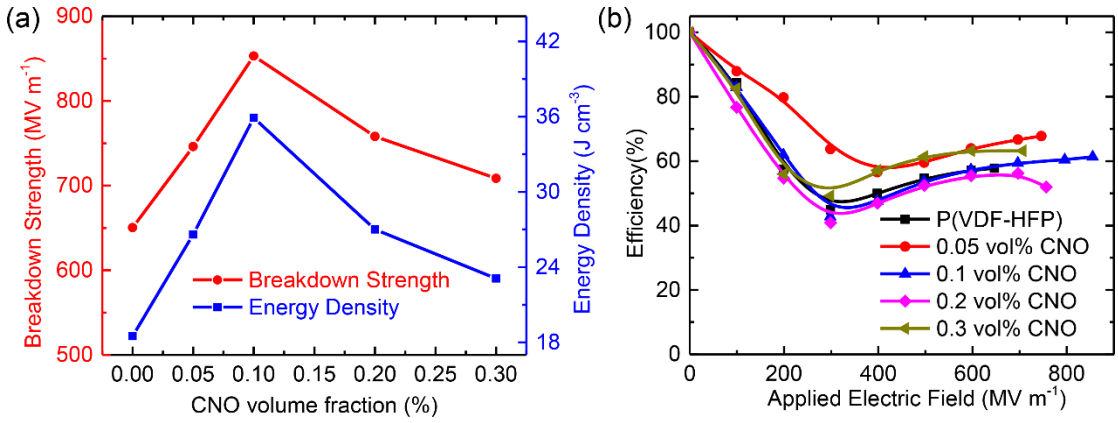

Supplementary Figure 8 Dielectric performance of polymer nanocomposite P(VDF-HFP)/$Ca_2Nb_3O_{10}$ (CNO) (a) The breakdown strength and energy density under different CNO volume fraction (b) The charge-discharge efficiency as a function of applied electric field.

References in Supplementary Information:

1. Zhang, X. *et al.* Polymer nanocomposites with ultrahigh energy density and high discharge efficiency by modulating their nanostructures in three dimensions. *Adv. Mater.* **30**, 1707269 (2018).

2. Jiang, Y. *et al.* Ultrahigh Breakdown Strength and Improved Energy Density of Polymer Nanocomposites with Gradient Distribution of Ceramic Nanoparticles. *Adv. Funct. Mater.* **30**, 1906112 (2020).

3. Zou, K. *et al.* Ultrahigh Energy Efficiency and Large Discharge Energy Density in Flexible Dielectric Nanocomposites with $Pb_{0.97}La_{0.02}(Zr_{0.5}Sn_xTi_{0.5-x})O_3$Antiferroelectric Nanofillers. *ACS Appl. Mater. Interfaces* **12**, 12847-12856 (2020).

4. Hu, P. *et al.* Topological-Structure Modulated Polymer Nanocomposites Exhibiting Highly Enhanced Dielectric Strength and Energy Density. *Adv. Funct. Mater.* **24**, 3172-3178 (2014).

5. Li, H. *et al.* Enabling High-Energy-Density High-Efficiency Ferroelectric Polymer Nanocomposites with Rationally Designed Nanofillers. *Adv. Funct. Mater.*, 2006739 (2020).

6. Wang, Y. *et al.* Significantly enhanced breakdown strength and energy density in sandwich-structured barium titanate/poly (vinylidene fluoride) nanocomposites. *Adv. Mater.* **27**, 6658-6663 (2015).

7. Tang, H., Lin, Y. & Sodano, H. A. Enhanced energy storage in nanocomposite capacitors through aligned PZT nanowires by uniaxial strain assembly. *Adv. Energy Mater.* **2**, 469-476 (2012).

8. Tang, H., Lin, Y. & Sodano, H. A. Synthesis of high aspect ratio $BaTiO_3$ nanowires for high energy density nanocomposite capacitors. *Adv. Energy Mater.* **3**, 451-456 (2013).

9. Jia, Q., Huang, X., Wang, G., Diao, J. & Jiang, P. MoS_2 nanosheet superstructures based polymer composites for high-dielectric and electrical energy storage applications. *J Phys. Chem. C* **120**, 10206-10214 (2016).

10. Pan, Z. *et al.* $NaNbO_3$ two-dimensional platelets induced highly energy storage density in trilayered architecture composites. *Nano Energy* **40**, 587-595 (2017).

11. Wen, R., Guo, J., Zhao, C. & Liu, Y. Nanocomposite capacitors with significantly enhanced energy density and breakdown strength utilizing a small loading of monolayer titania. *Adv. Mater. Interfaces* **5**, 1701088 (2018).

12. Tang, H. & Sodano, H. A. Ultra high energy density nanocomposite capacitors with fast discharge using $Ba_{0.2}Sr_{0.8}TiO_3$ nanowires. *Nano Lett.* **13**, 1373-1379 (2013).

13. Kim, P. *et al.* High energy density nanocomposites based on surface-modified $BaTiO_3$ and a ferroelectric polymer. *ACS nano* **3**, 2581-2592 (2009).

14. Li, Q. *et al.* Solution-processed ferroelectric terpolymer nanocomposites with high breakdown strength and energy density utilizing boron nitride nanosheets. *Energ. Environ. Sci.* **8**, 922-931 (2015).

15. Wang, G., Huang, X. & Jiang, P. Mussel-inspired fluoro-polydopamine functionalization of titanium dioxide nanowires for polymer nanocomposites with significantly enhanced energy storage capability. *Sci. Rep.* **7**, 43071 (2017).